ELSEVIER

Polymer 44 (2003) 995–1001

polymer

www.elsevier.com/locate/polymer

High-permeability fluorinated polyimide microcapsules by vapor deposition polymerization

F.Y. Tsai[a,b], D.R. Harding[a,b,*], S.H. Chen[a,b], T.N. Blanton[c]

[a]*Laboratory for Laser Energetics, University of Rochester, 250 East River Road, Rochester, NY 14623-1299, USA*
[b]*Department of Chemical Engineering, University of Rochester, 250 East River Road, Rochester, NY 14623-1299, USA*
[c]*Eastman Kodak Company, Research and Development Laboratories, Rochester, NY 14650-2106, USA*

Received 26 July 2002; received in revised form 22 October 2002; accepted 24 October 2002

Abstract

Spherical microcapsules (~1 mm in diameter and ~1 μm in wall thickness) to be used as inertial confinement fusion targets were prepared from 6FDA–ODA polyimide by vapor deposition polymerization. Compared with the previously developed PMDA–ODA polyimide microcapsules, the 6FDA–ODA microcapsules were ~50-fold more permeable to gases including He, D_2, O_2, N_2, Ar, and Ne, considerably more transparent in the UV–visible spectrum, and of marginally lower Young's modulus, tensile strength, and elongation at break. The microcapsules possessed amorphous morphology with an amorphous *d*-spacing of 5.8 Å as determined by wide-angle X-ray diffraction. The cryogenic permeability of helium was measured between 133 and 295 K, and the activation energy for permeation was determined to be 12.3 kJ/mol.

Keywords: Vapor deposited polyimide; Inertial confinement fusion; Fluorinated polyimide

1. Introduction

Spherical, thin-walled microcapsules are used as targets that hold deuterium–tritium (DT) fuel in inertial confinement fusion (ICF) experiments [1,2]. An optimal design of the ICF target consists of a microcapsule, 1 mm in diameter and 1 μm in wall thickness, and a concentric 100 μm thick layer of solidified DT adhered to the inner capsule surface. The process to prepare such targets typically involves (1) filling the microcapsules with DT gas by permeation to 1000 atm at room temperatures, (2) cooling to below 20 K to solidify the DT, and (3) maintaining the capsule at an isotherm of 19 K to allow the solid DT layer to redistribute itself into a uniform layer. These procedures call for microcapsules that can withstand rapid filling and cooling without buckling or bursting from the pressure differential created therein, and that allow optical characterization of the resulting solid DT layer. The desired material properties for microcapsules, therefore, include high gas permeability, high Young's modulus and tensile strength, and good optical transparency [1–4]. Recent developments in target fabrication for ICF have established the production of poly(4,4′-oxydiphenylpyromellitimide) (PMDA–ODA polyimide) microcapsules [3,5–8] via vapor deposition polymerization (VDP) [9,10] to take advantage of the excellent mechanical properties. PMDA–ODA polyimide, however, possesses relatively low gas permeability that makes it time consuming to fill and cool the microcapsules [7,8]. Long filling and cooling procedures have an adverse effect on ICF experiments, because they increase the buildup of He [3] in the targets from tritium decay, which greatly reduces the yield of the fusion reaction [11,12].

Fluorinated polyimides are known to offer distinct properties including high gas permeability and low optical absorption while still retaining good mechanical properties [13], which will be highly desirable for the ICF application. One of the widely investigated fluorinated polyimides is 6FDA–ODA polyimide polymerized from 4,4′-(hexafluoroisopropylidene)diphthalic-anhydride (6FDA) and 4,4′-oxydianiline (ODA). Based on the literature properties of solution-cast 6FDA–ODA polyimide [14,15], it was expected that a 6FDA–ODA microcapsule would be capable of being filled and cooled up to 30-fold more

* Corresponding author. Address: Department of Chemical Engineering, University of Rochester, 250 East River Road, Rochester, NY 14623-1299, USA. Tel.: +1-585-275-5850; fax: +1-585-275-5960.
E-mail address: dhar@lle.rochester.edu (D.R. Harding).

0032-3861/03/$ - see front matter © 2002 Elsevier Science Ltd. All rights reserved.
PII: S0032-3861(02)00787-5

rapidly than a PMDA–ODA capsule. In this study, we adopted the previously established vapor deposition process for producing PMDA–ODA polyimide microcapsules to develop 6FDA–ODA microcapsules, which were characterized to determine the gas permeability, Young's modulus, tensile strength, elongation at break, and other physical and chemical properties.

2. Experimental

2.1. Materials

6FDA, purchased from Lancaster Chemicals (99% purity), was used as received; ODA (99 + % purity; zone refined), purchased from Aldrich Chemical, was ground into fine powder using a mortar before being used. Spherical poly(α-methyl styrene) (PAMS) shells ($M_w = 400\,000$) (~935 μm in diameter and 7.5–17 μm in wall thickness) were received from General Atomics and used without further treatment. Sodium chloride disks (13 mm in diameter and 1 mm in wall thickness) were purchased from International Crystal Laboratories.

2.2. Fabrication

Polyimide microcapsules were prepared by a two-step process: (1) 6FDA and ODA monomers were sublimed in vacuum into vapors, which polymerized into poly(amic acid) on the surface of PAMS shells being mechanically agitated; the purpose of agitation was to ensure uniform coating on the entire surface of the PAMS shells, (2) the coated shells were thermally cured to convert poly(amic acid) into polyimide (imidization). Meanwhile, the PAMS shells decomposed at elevated temperatures into gaseous products that permeated through the polyimide layer, leaving behind freestanding polyimide capsules. The deposition conditions were as follows: subliming temperature: 6FDA = 181 °C and ODA = 135 °C; deposition pressure = 5×10^{-6} Torr; monomer preheat = 30 min. The resultant deposition rate was ~7 μm/h on spheres and ~15 μm/h on flat films. Imidization was carried out in an NEY Centurion VPM furnace with programmable temperatures (accuracy = ±0.1 °C). The furnace was purged with a constant flow of nitrogen (7.5 standard cm^3/min) throughout imidization. The temperature cycle for imidization consisted of three steps: (1) heating from 25 to 300 °C at 0.1 °C/min; (2) soaking at 300 °C for 3 h; and (3) cooling to 25 °C at 5 °C/min. The reaction scheme of the formation of polyimide is shown in Fig. 1.

Flat films were prepared similarly, except that sodium chloride disks were used as substrates, which were dissolved in de-ionized water after imidization. The freestanding polyimide films that remained were vacuum-dried at 80 °C for 24 h. Detailed descriptions of the fabrication process and the fabrication conditions for PMDA–ODA polyimide films and microcapsules can be found elsewhere [3,8].

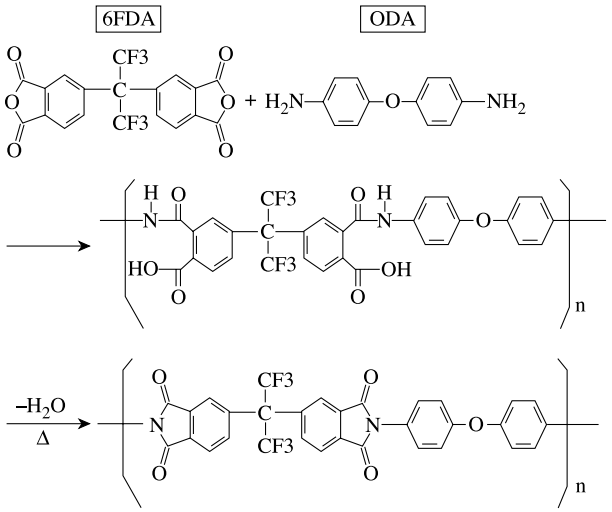

Fig. 1. Chemical structure and reaction scheme of 6FDA–ODA polyimide.

2.3. Chemical and morphological characterization

Fourier transform infrared (FTIR) spectra were acquired on both as-deposited and imidized film samples attached to a sodium chloride disk using a Nicolet 20SXC FTIR spectrometer. The glass transition temperature (T_g) was determined using a Perkin–Elmer DSC7 differential scanning calorimeter with a 20 °C/min heating rate.

Wide-angle X-ray diffraction measurements were conducted in the transmission and reflection modes [16]. A Rigaku D2000 Bragg–Brentano diffractometer [17] equipped with a copper rotating anode, diffracted beam graphite monochromator, and scintillation detector was used to obtain reflection-mode diffraction patterns. Data were collected as continuous scans at a scan rate of 2° 2θ/min. A Bruker AXS microdiffractometer [18] equipped with a copper rotating anode, Goebel mirrors, a 0.5 mm collimator, and a two-dimensional general area detector diffraction system (GADDS) was used to obtain transmission-mode patterns. Each microdiffractometer data set was collected until 10^7-total-counts integrated intensity was achieved.

The density was measured using a Techne TE-10A density column with an aqueous zinc chloride solution. The samples were allowed 24 h in the column to settle into the equilibrium position. The measurements were performed by General Atomics to an accuracy of 0.001 g/cm^3.

2.4. Mechanical properties

The mechanical properties of the microcapsules were determined from buckle and burst tests, where the microcapsules were exposed to a uniform pressure differential of helium or nitrogen across the capsule wall to cause

buckling or bursting. The Young's modulus is related to the buckling pressure differential as given by [19]

$$P_{\text{buckle}} = \frac{2E}{\sqrt{3(1-\nu^2)}}\left(\frac{w}{r}\right)^2, \quad (1)$$

where E is the Young's modulus, ν the Poisson's ratio (~ 0.34), P_{buckle} the buckling pressure differential, and r and w the radius and wall thickness of the capsule, respectively. The tensile strength is proportional to the bursting pressure differential as given by [19]

$$P_{\text{burst}} = 2\sigma\frac{w_b}{r_b}, \quad (2)$$

where P_{burst} is the bursting pressure differential, σ the tensile strength, and r_b and w_b the capsule radius and wall thickness immediately prior to bursting. The elongation at break under biaxial strain is given by

$$\varepsilon = \frac{r_b}{r_0} - 1, \quad (3)$$

where ε is the elongation at break and r_0 is the initial capsule radius. Detailed descriptions of the experimental setups and procedures can be found elsewhere [3,8].

2.5. Gas permeability

The gas permeability was determined by two methods: (1) permeation time constant measurements with microcapsules and (2) measurements based on ASTM D1434-82 with hemispherical samples prepared by splitting microcapsules in half. The former method was used for room-temperature testing only, while the latter was used for cryogenic-temperature measurements. The test gases included helium, deuterium, oxygen, nitrogen, argon, and neon. Detailed descriptions of the experimental setups and procedures can be found elsewhere [3,16,20].

3. Results and discussion

3.1. Fabrication and characterization

The FTIR spectra of the as-deposited poly(amic acid) and cured polyimide are shown in Fig. 2. The as-deposited spectrum contained both the poly(amic acid) characteristic peaks at 1710 (C=O in COOH), 1660 (C=O in CONH), and 1550 (C–NH) cm^{-1} and the monomer peaks at 1820 (C=O) and 1780 (C=O) for 6FDA and ~3200 (NH_2) cm^{-1} for ODA [21]. The characteristic peaks of polyimide [21] at 1790 (C=O asymmetric stretching), 1720 (C=O symmetrical stretching), and 1380 (C–N stretching) cm^{-1} appear upon imidization with the monomer peaks becoming unobservable. The spectra indicate that the unreacted monomers in the as-deposited samples were polymerized with complete conversion and/or desorbed upon thermal imidization.

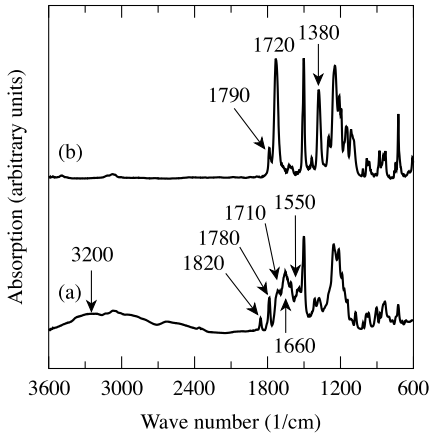

Fig. 2. FTIR spectra of (a) as-deposited 6FDA–ODA poly(amic acid) and (b) polyimide. Curve (a) contains absorption peaks corresponding to poly(amic acid): 1710, 1660, and 1550 cm^{-1}; 6FDA: 1820 and 1780 cm^{-1}; ODA: 3200 cm^{-1}. Curve (b) contains the polyimide characteristic peaks at 1790, 1720, and 1380 cm^{-1}.

The 6FDA–ODA capsules were observed to possess a relatively rough surface compared with that of the PMDA–ODA capsules, as shown in the SEM surface micrographs in Fig. 3. The higher surface roughness may be attributed to the low surface adhesion of 6FDA–ODA [22], which may render the nascent surface during deposition susceptible to

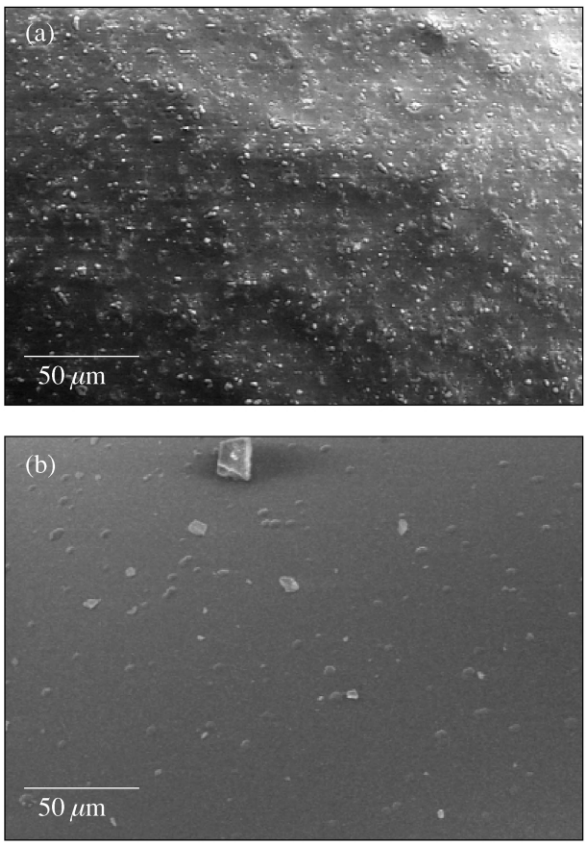

Fig. 3. SEM micrographs of the surfaces of (a) 6FDA–ODA and (b) PMDA–ODA polyimide microcapsules.

abrasion damages induced by the shells' agitation and collision motions [23]. The weak adhesion of 6FDA–ODA is attributed to the bulky fluorocarbon groups that reduce the chain mobility crucial to the surface-bonding mechanism of polymers, as interpenetration and diffusion of polymer chains between surfaces are prerequisite for strong adhesion [22].

The survivability of the microcapsules in imidization was strongly dependent on the decomposition behavior of the PAMS shells, which decompose into gaseous products to create internal overpressures that can inflate and burst the capsules. The 6FDA–ODA capsules showed a stronger tendency to burst than the PMDA–ODA capsules during imidization. Fig. 4 displays the diameter of 6FDA–ODA capsules changing as a function of temperature during imidization, with the equivalent data for PMDA–ODA for comparison. The 6FDA–ODA capsules inflated to a greater extent than the PMDA–ODA capsules, indicating that 6FDA–ODA polyimide was softer at elevated temperatures. This observation is consistent with 6FDA–ODA's lower T_g value determined by DSC, as shown in Fig. 5: the 6FDA–ODA had a T_g of 320 °C while the T_g of PMDA–ODA is reported to be ~400 °C [24]. The relative softness of 6FDA–ODA necessitated a slow heating rate, 0.1 °C/min, and thin-walled PAMS shells (7.5 μm) to achieve 100% capsule survivability in imidization. Note that thinner PAMS shells have less mass, which when decomposed creates lower overpressure.

Fig. 6 displays the X-ray diffraction pattern of the vapor-deposited 6FDA–ODA polyimide. Both the reflection- and transmission-mode patterns suggest amorphous morphology: the reflection-mode pattern is characterized by one broad diffraction band at ~15.3° 2θ, indicating that the samples were amorphous; the transmission-mode diffraction pattern shows a uniform scattering, indicating that there was

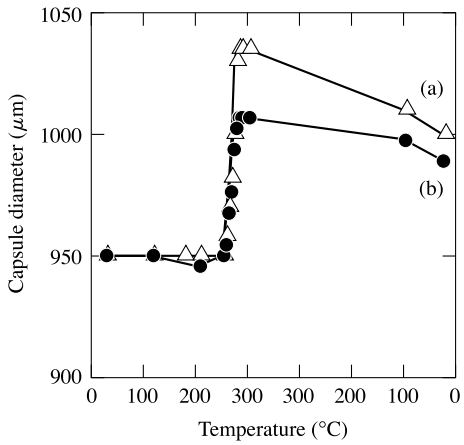

Fig. 4. Changes in the diameter of (a) 6FDA–ODA and (b) PMDA–ODA microcapsules during imidization. The capsules inflated as PAMS mandrels decomposed to create internal overpressures. The greater inflation of the 6FDA–ODA capsules indicated their relative softness at elevated temperature. The imidization conditions were as described in experimental. The PAMS mandrels used were 17 μm in wall thickness.

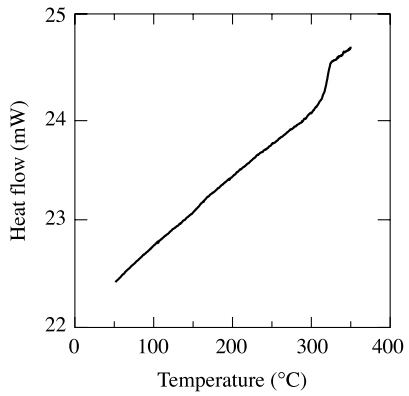

Fig. 5. Differential scanning calorimetry (DSC) data acquired with vapor-deposited 6FDA–ODA polyimide samples. The T_g is at 320 °C with $\Delta C_p = 0.22$ J/g °C. The heating rate was 20 °C/min.

no preferred orientation of the polymer chains. The *d*-spacing corresponding to the amorphous diffraction peak at ~15.3° 2θ was calculated using Bragg's law to be 5.8 Å, which agrees with the literature value for solution-cast 6FDA–ODA [14]. The amorphous state can be expected based on the chemical structure of 6FDA–ODA, where the bulky and rigid fluorocarbon groups prevent long-range chain motions that are required for crystallization and orientation.

The UV–visible spectra of 6FDA–ODA and PMDA–ODA polyimide in Fig. 7 show that the 6FDA–ODA was considerably more transparent in the measured wavelength range.

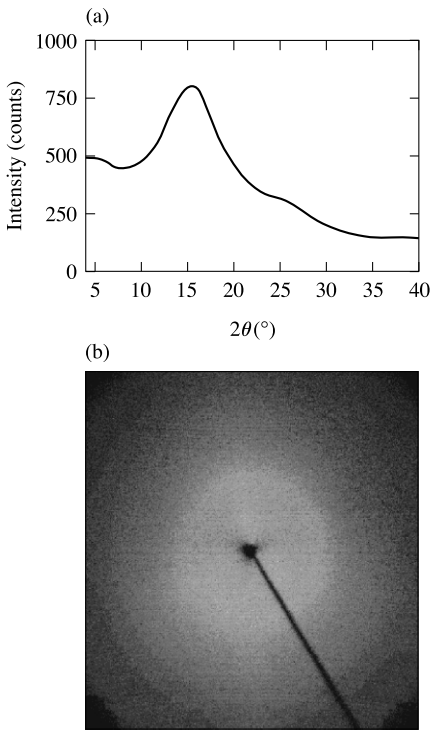

Fig. 6. (a) Reflection- and (b) transmission-mode X-ray diffraction patterns of vapor-deposited 6FDA–ODA polyimide.

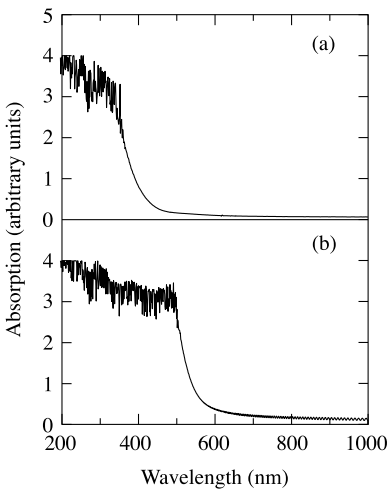

Fig. 7. UV–visible spectra of (a) 6FDA–ODA and (b) PMDA–ODA vapor-deposited polyimide.

3.2. Mechanical and permeation properties

The gas permeability, Young's modulus, tensile strength, and elongation at break of the 6FDA–ODA polyimide microcapsules are listed in Table 1 and compared with the reported values for PMDA–ODA microcapsules [3,16,25]. The mechanical properties of 6FDA–ODA polyimide were ~20% lower than those of PMDA–ODA; however, its permeability was a factor of ~50 higher. The actual mechanical properties of the 6FDA–ODA capsules could have been of higher values since their rougher surfaces furthered the deviation from perfect spheres, which may have lowered their bursting and buckling pressure differentials. Table 2 summarizes the performances of 6FDA–ODA and PMDA–ODA microcapsules (1 mm diameter and 1 μm wall) as ICF targets [25]. Owing to their high permeability, the 6FDA–ODA microcapsules can be filled ~40-fold faster and cooled more rapidly, a significant improvement for the ICF application.

Table 3 compares the permeability and density of the vapor-deposited 6FDA–ODA polyimide with the literature values for solution-cast polyimide [14,15]. The vapor-deposited polyimide possessed ~40% higher gas permeability, which may be attributed to its lower density, as lower density indicates a higher content of free volume that expedites permeation in polymers [26]. The lower density of the vapor-deposited 6FDA–ODA may be attributed to the absence of solvents in the fabrication process; i.e. without solvents acting as plasticizers, the polymer chains with bulky fluorocarbon side groups possess little mobility to rearrange and settle into a high packing density.

Table 1
Properties of vapor-deposited 6FDA–ODA polyimide microcapsules compared with corresponding value for PMDA–ODA microcapsules

	Mechanical properties			Gas permeability (mol m/m^2 Pa s)				E_P (helium) (kJ/mol)
	E (GPa)	σ (MPa)	ε	He × 10^{16}	D_2 × 10^{16}	O_2 × 10^{17}	N_2 × 10^{18}	
6FDA–ODA	2.6 ± 0.1	221 ± 15	0.15 ± 0.02	194 ± 8	165 ± 9	198 ± 9	351 ± 10	12.3 ± 0.7
PMDA–ODA ([3,16,25])	3.2 ± 0.1	280 ± 19	0.27 ± 0.02	4.9 ± 0.1	3.5 ± 0.1	1.7 ± 0.2	3.9 ± 0.2	20.1 ± 0.2

The property values were averaged from the experimental results of ~100 microcapsule samples. The error values represent the 95% confidence intervals.

Table 2
Performances of 6FDA–ODA and PMDA–ODA polyimide microcapsules (1 mm diameter and 1 μm wall thickness) as ICF targets

	D_2 time constants (s)[a]	Maximum fill rate (atm/min)	Fill time to 1000 atm with D_2 (h)	Buckling pressure (atm)	Burst pressure (atm)
6FDA–ODA	4.1	1.90	8.8	0.13	8.7
PMDA–ODA [25]	194.2	0.05	333.3	0.16	11.1

[a] The time constant represents the length of time required for a filled capsule to reduce to 36.8% ($1/e$) of its initial pressure after being placed in a vacuum environment, as a result of permeation [20].

Table 3
Gas permeability of vapor-deposited 6FDA–ODA polyimide compared with the literature values for solution-cast polyimide

	Gas permeability (mol m/m^2 Pa s) × 10^{16}						Density (g/cm^3)
	He	D_2	Ne	Ar	O_2	N_2	
Vapor-deposited	194	165	43	6.3	19.8	3.5	1.423
Solution-cast	172 [14]				13.0 [15]	2.5 [15]	1.432 [15]

Note that the literature permeability values were measured at 35 °C while the vapor-deposited values were measured at 22 °C. The permeability of the solution-cast polyimide would be lower at 22 °C.

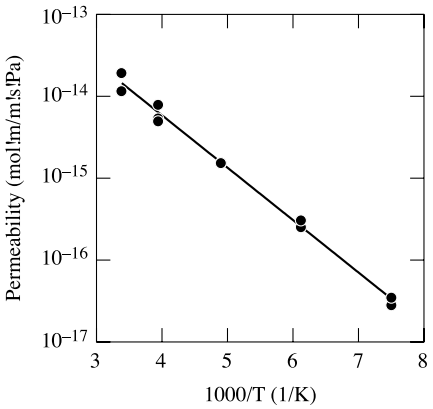

Fig. 8. Temperature dependency of the helium permeability through vapor-deposited 6FDA–ODA polyimide microcapsules. The activation energy for permeation was 12.3 kJ/mol.

The temperature dependency of the helium permeability of 6FDA–ODA microcapsules between 133 and 295 K is displayed in Fig. 8. The permeability-temperature data follows the Arrhenius' relationship with an activation energy for permeation (E_P) of 12.3 kJ/mol, which is considerably lower than the reported value of 20.1 kJ/mol for PMDA–ODA microcapsules [16,25] as shown in Table 1. The lower activation energy for permeation of the 6FDA–ODA polyimide indicates higher segmental mobility [27,28], which may be explained in terms of the chemical structures. The activation energy for permeation of aromatic polyimides such as PMDA–ODA and 6FDA–ODA is mainly dependent on the localized segmental motions such as the rotational motions of the 'spacer' groups between the rigid phenyl rings [26]. In PMDA–ODA, the flexible ether link in ODA is responsible for most of the rotational motions, as the planer PMDA moieties have little mobility. In 6FDA–ODA, the 6FDA moieties allow some rotational motions in the $-C(CF_3)_2-$ groups in addition to the ether link in ODA, thereby increasing the total rotational motions and lowering the activation energy for permeation.

4. Conclusion

The plausibility of modifying the chemical structure to achieve desirable properties of polyimide microcapsules for the ICF application has been demonstrated. Using the same vapor deposition process, changing the dianhydride monomer from PMDA to 6FDA increased the gas permeability of the resultant polyimide capsules by a factor of ~50 with marginal reductions in the mechanical properties. The 6FDA–ODA polyimide microcapsules can be filled ~40-fold faster and cooled more rapidly when used as ICF targets. The higher permeability of the vapor-deposited 6FDA–ODA compared with the literature value for solution-cast 6FDA–ODA was attributed to the higher free volume content resulting from the solvent-less fabrication process, where the chain mobility was limited to prevent close-packing. The cryogenic permeability of 6FDA–ODA followed the Arrhenius' relation between 133 and 295 K with lower activation energy for permeation than that of PMDA–ODA polyimide due to the added segmental mobility by the fluorocarbon groups. The low adhesion and relatively low T_g of 6FDA–ODA increased the capsule surface roughness and lowered the survivability in imidization, respectively.

Acknowledgements

This work was supported by the US Department of Energy Office of Inertial Confinement Fusion under Cooperative Agreement No. DE-FC03-92SF19460, the University of Rochester, and the New York State Energy Research and Development Authority. The support of DOE does not constitute an endorsement by DOE of the views expressed in this article.

References

[1] Schultz KR, Kaae JL, Miller WJ, Steinman DA, Stephens RB. Fusion Engng Des 1999;44:441.
[2] Schultz KR. In: Miley GH, Elliot C, editors. 16th IEEE/NPSS Symposium Fusion Engineering, SOFE'95, vol. 1. New York: IEEE; 1995. p. 116.
[3] Tsai F-Y, Alfonso EL, Harding DR, Chen SH. J Phys D: Appl Phys 2001;34:3011.
[4] Letts SA, Fearon EM, Buckley SR, Saculla MD, Allison LM, Cook R. Fusion Technol 1995;28:1797.
[5] Alfonso EL, Chen SH, Gram RQ, Harding DR. J Mater Res 1998;13:2988.
[6] Roberts CC, Letts SA, Saculla MD, Hsieh EJ, Cook RC. Fusion Technol 1999;35:138.
[7] Tsai F-Y, Alfonso EL, Chen S-H, Harding DR. Fusion Technol 2000;38:83.
[8] Tsai F-Y, Harding DR, Chen SH, Blanton TN, Alfonso EL. J Fusion Sci Technol 2002;41:178.
[9] Salem JR, Sequeda FO, Duran J, Lee WY, Yang RM. J Vac Sci Technol A 1986;4:369.
[10] Iijima M, Takahashi Y, Inagawa K, Itoh A. J Vac Sci Jpn 1985;28:437.
[11] Town RPJ. LLE. Private communication.
[12] Larsen JT. J Vac Sci Technol 1989;7:1150.
[13] Sasaki S, Nishi S. In: Ghosh MK, Mittal KL, editors. Polyimides: fundamentals and applications. Plastics engineering, vol. 36. New York: Marcel Dekker; 1996. p. 71.
[14] Kim TH, Koros WJ, Husk GR, O'Brien KC. J Membr Sci 1988;37:45.
[15] Tanaka K, Kita H, Okano M, Okamoto K. Polymer 1992;33:585.
[16] Tsai F-Y, Blanton TN, Harding DR, Chen SH. Temperature dependency of the properties of vapor-deposited polyimide. Submitted for publication.
[17] Jenkins R, Snyder RL. Introduction to X-ray powder diffractometry. New York: Wiley; 1996. Chapter 7, p. 173.
[18] Squires BA, Smith KL. In: Predecki PK, Gilfrich JV, Huang TC, Noyan IC, Bowen DK, Goldsmith CC, Jenkins R, Smith DK, editors. Advances in X-ray analysis, vol. 38. New York: Plenum Press; 1995. p. 511.
[19] Young WC. Roark's formulas for stress & strain, 6th ed. New York: McGraw-Hill; 1989. Chapter 13, p. 647.

[20] Bonino M, Gram RQ, Harding D, Noyes S, Soures J, Wittman M. Retention of D_2 and DT in plastic shell targets using thin aluminum. Presented at the Eleventh Target Fabrication Specialists' Meeting, Orcas Island, WA; 9–12 September 1996.
[21] Takekoshi T. In: Ghosh MK, Mittal KL, editors. Polyimides: fundamentals and applications. Plastics engineering, vol. 36. New York: Marcel Dekker; 1996. p. 7.
[22] Maier G. Prog Polym Sci 2001;26:3.
[23] Roberts CC, Orthion PJ, Hassel AE, Parrish BK, Buckley SR, Fearon E, Letts SA, Cook RC. Fusion Technol 2000;38:94.
[24] Megusar J. J Nucl Mater 1997;245:185.
[25] Tsai F-Y. PhD Thesis. University of Rochester; 2002.
[26] Stern SA. J Membr Sci 1994;94:1.
[27] Singh-Ghosal A, Koros WJ. Ind Engng Chem Res 1999;38:3647.
[28] Hedenqvist M, Gedde UW. Prog Polym Sci 1996;21:299.